

## Supporting Information

### Photogenerated aryl mesylate and aryl diethyl phosphate radical cations. A time-resolved spectroscopy investigation.

Sergio M. Bonesi,<sup>[a],[b],[c]\*</sup> Stefano Protti,<sup>[a]</sup> Andrea Capucciati,<sup>[d]</sup> Maurizio Fagnoni<sup>[a]</sup>

<sup>[a]</sup>PhotoGreen Lab, Department of Chemistry, University of Pavia, V.le Taramelli 12, 27100 Pavia, Italy.

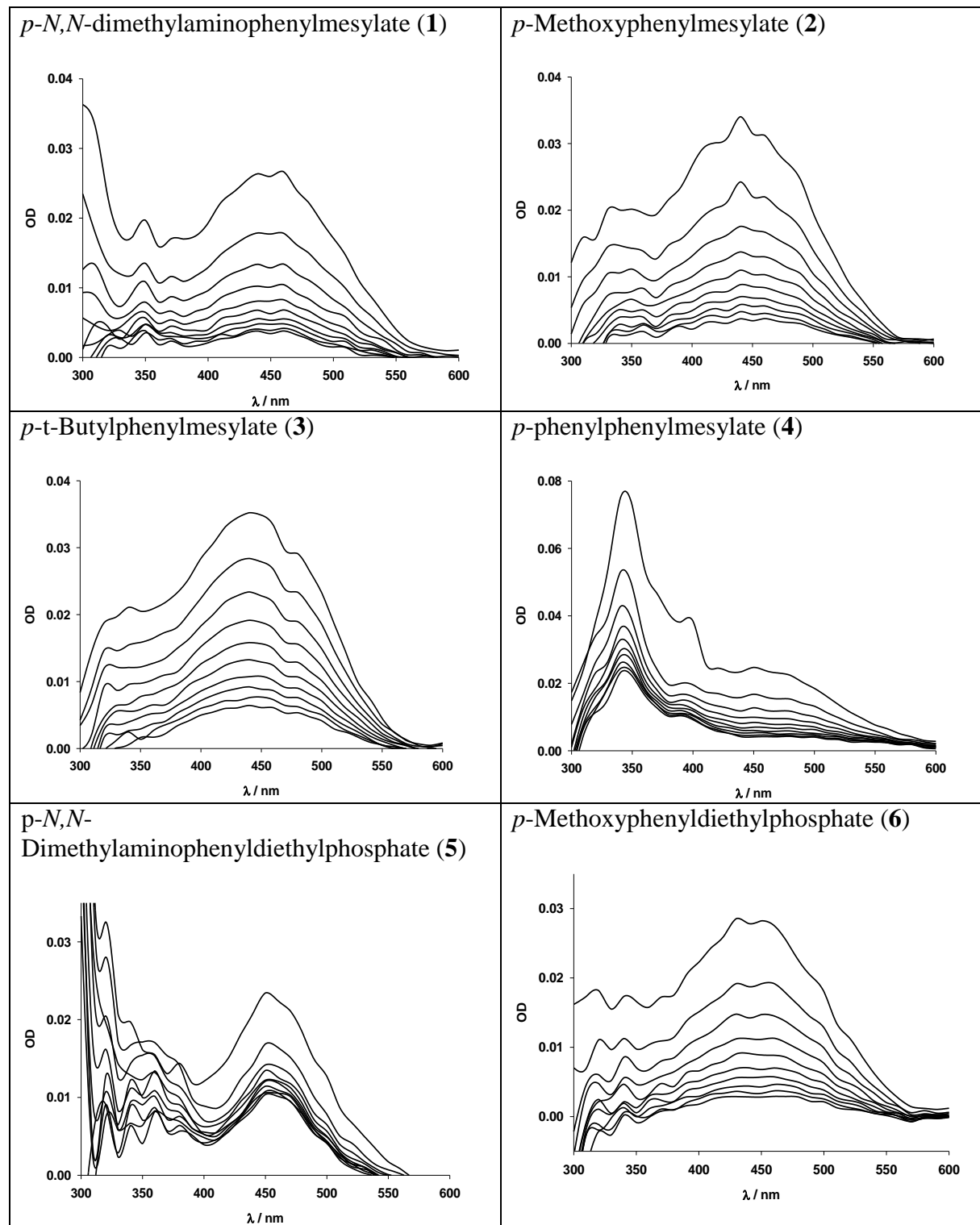
<sup>[b]</sup>Universidad de Buenos Aires. Departamento de Química Orgánica, Facultad de Ciencias Exactas y Naturales, Ciudad Universitaria, Buenos Aires, C1428EGA (Argentina).

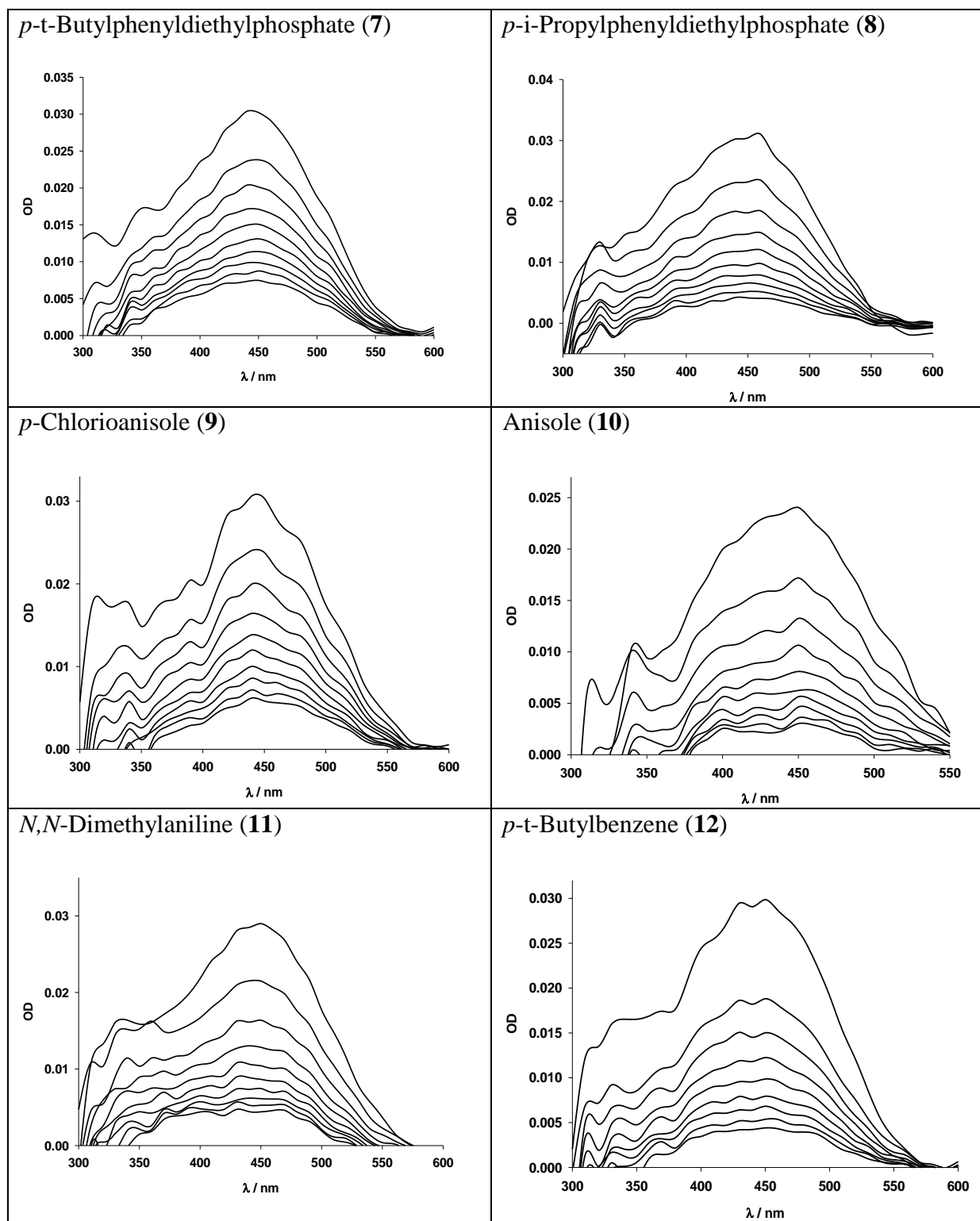
<sup>[c]</sup>CONICET—Universidad de Buenos Aires. Centro de Investigaciones en Hidratos de Carbono (CIHIDECAR). Ciudad Universitaria, Buenos Aires, C1428EGA (Argentina).

<sup>[d]</sup>Department of Chemistry, V.le Taramelli 12, 27100 Pavia, Italy

Corresponding author: [smbonesi@qo.fcen.uba.ar](mailto:smbonesi@qo.fcen.uba.ar)

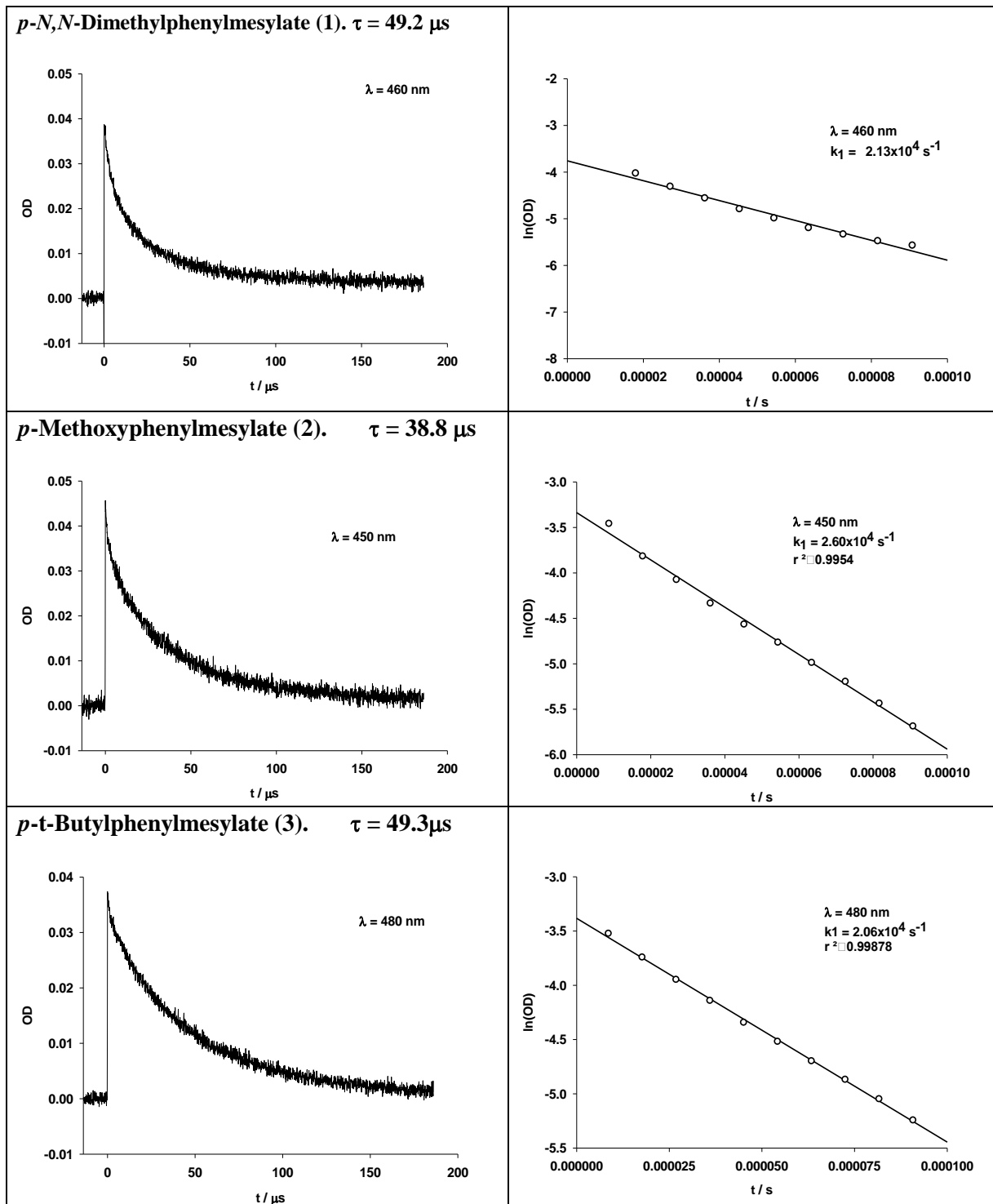
Index	Pages
1. Time-resolved UV-visible absorption spectra of aryl mesylates (1 – 4) and aryl phosphates (5 – 8).	S2
2. Transient decay traces and linear correlation plots with regression fittings.	S4
3. Solvent effect on the fragmentation rate constants of radical cations.	S8
4. Hammett linear correlations of the fragmentation rate constants ( $k_{\text{frag}}$ ) of radical cations and electron-transfer rate constants ( $k_{\text{ET}}$ ) of esters 1 - 8.	S8
5. Quenching of radical cation decay traces by addition of increasing concentration of $\text{NaN}_3$ .	S9
6. Measurement of extinction coefficients ( $\epsilon$ ) and quantum yield of formation ( $\phi$ ) of radical cations and calculation of the electron-transfer rate constants ( $k_{\text{ET}}$ ).	S10
7. References.	S13

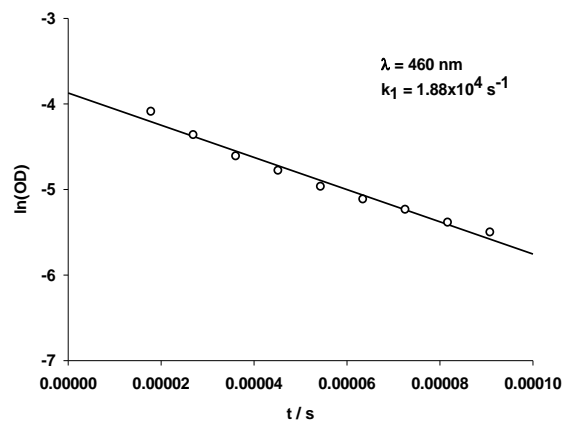
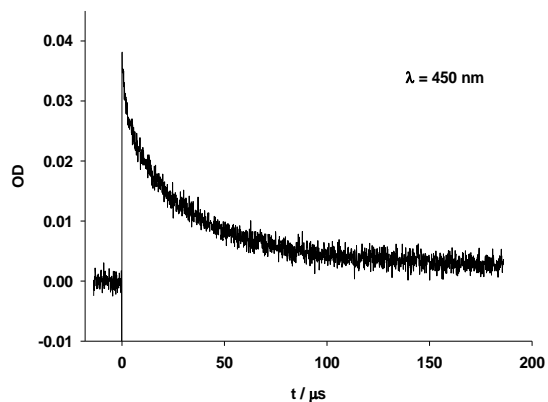
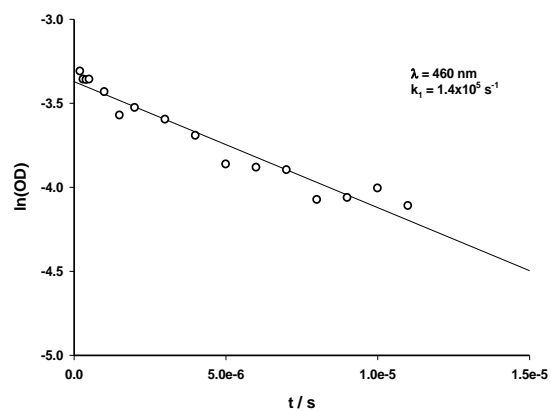
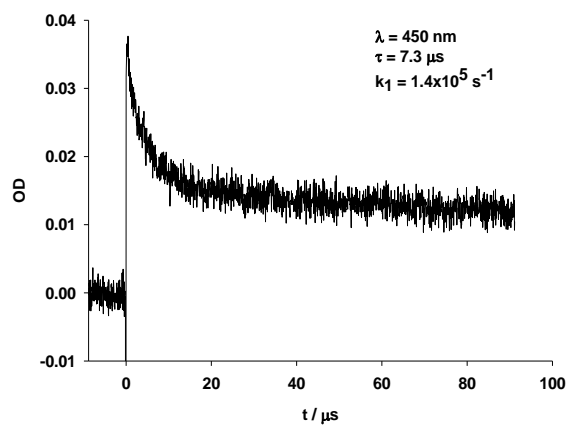
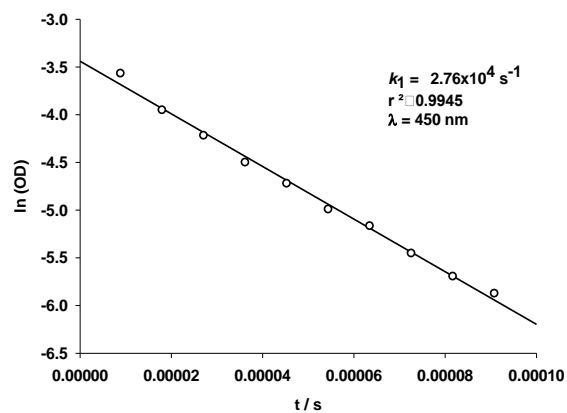
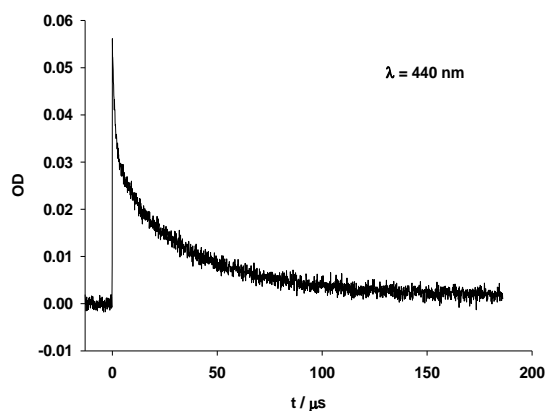
**1. Time-resolved UV-visible absorption spectra of aryl mesylates (1 – 4) and aryl phosphates (5 – 8).**

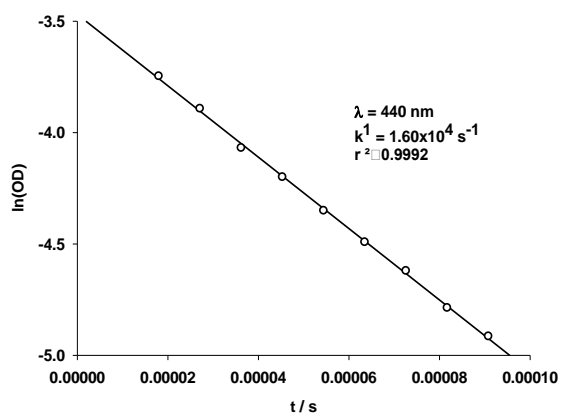
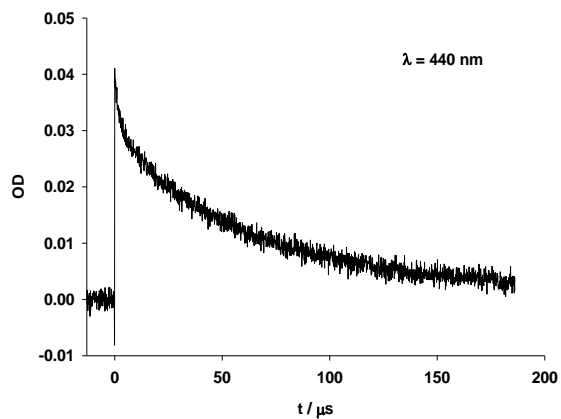
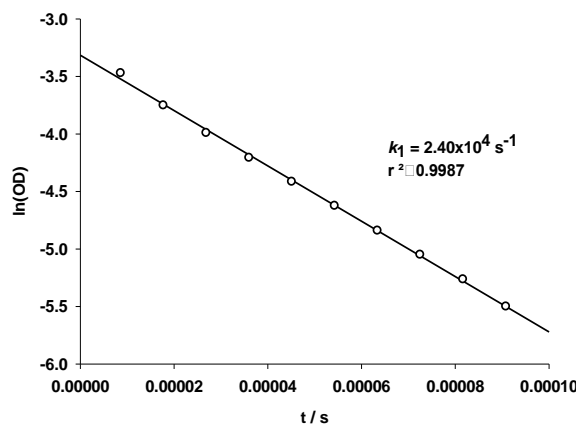
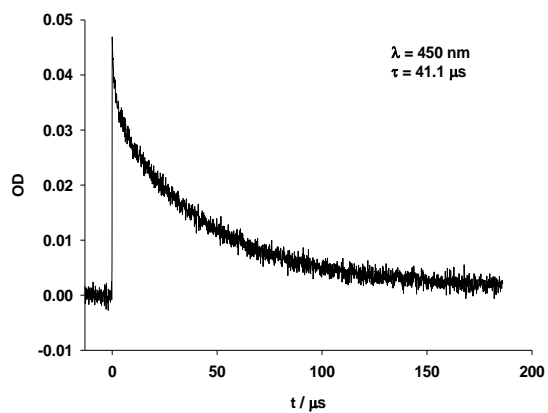
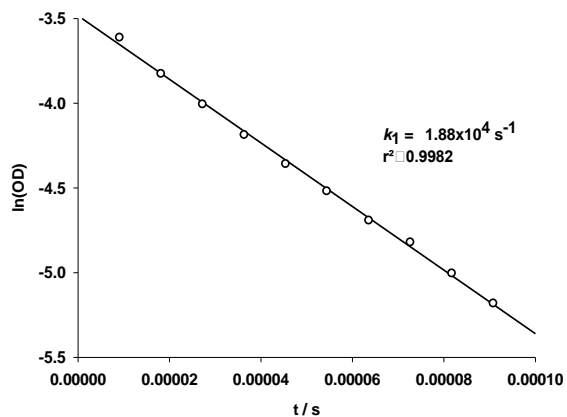
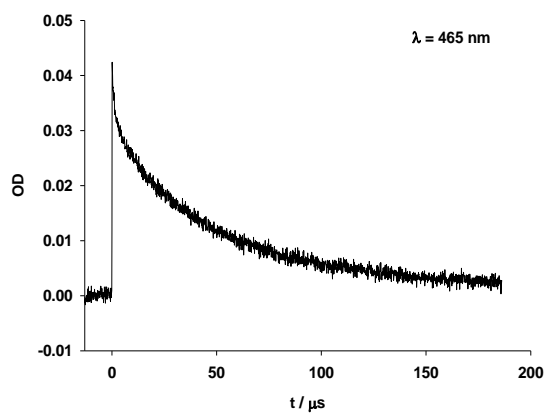


**Figure S1.** Time-resolved UV-vis spectra of radical cations of aryl mesylates (1–4), aryl phosphates (5–8), *p*-chloroanisole (9), anisole (10), *N,N*-dimethylaniline (11) and *p*-t-butylbenzene (12) in the presence of ammonium persulfate in MeCN/H<sub>2</sub>O (9:1) under N<sub>2</sub> atmosphere. Window time: 10–100  $\mu$ s.

## 2. Transient decay traces and linear correlation plots with regression fittings.



***p*-Phenylphenylmesylate (4).  $\tau = 53.2\mu\text{s}$** ***p*-*N,N*-Dimethylphenyldiethylphosphate (5).  $\tau = 7.3\mu\text{s}$** ***p*-Methoxyphenyldiethylphosphate (6).  $\tau = 36.2\mu\text{s}$** 

***p*-t-Butylphenyldiethylphosphate (7).  $\tau = 61.9\mu\text{s}$** ***p*-i-Propylphenyldiethylphosphate (8).  $\tau = 41.1\mu\text{s}$** ***p*-Cloroanisole (9).  $\tau = 49.7\mu\text{s}$** 

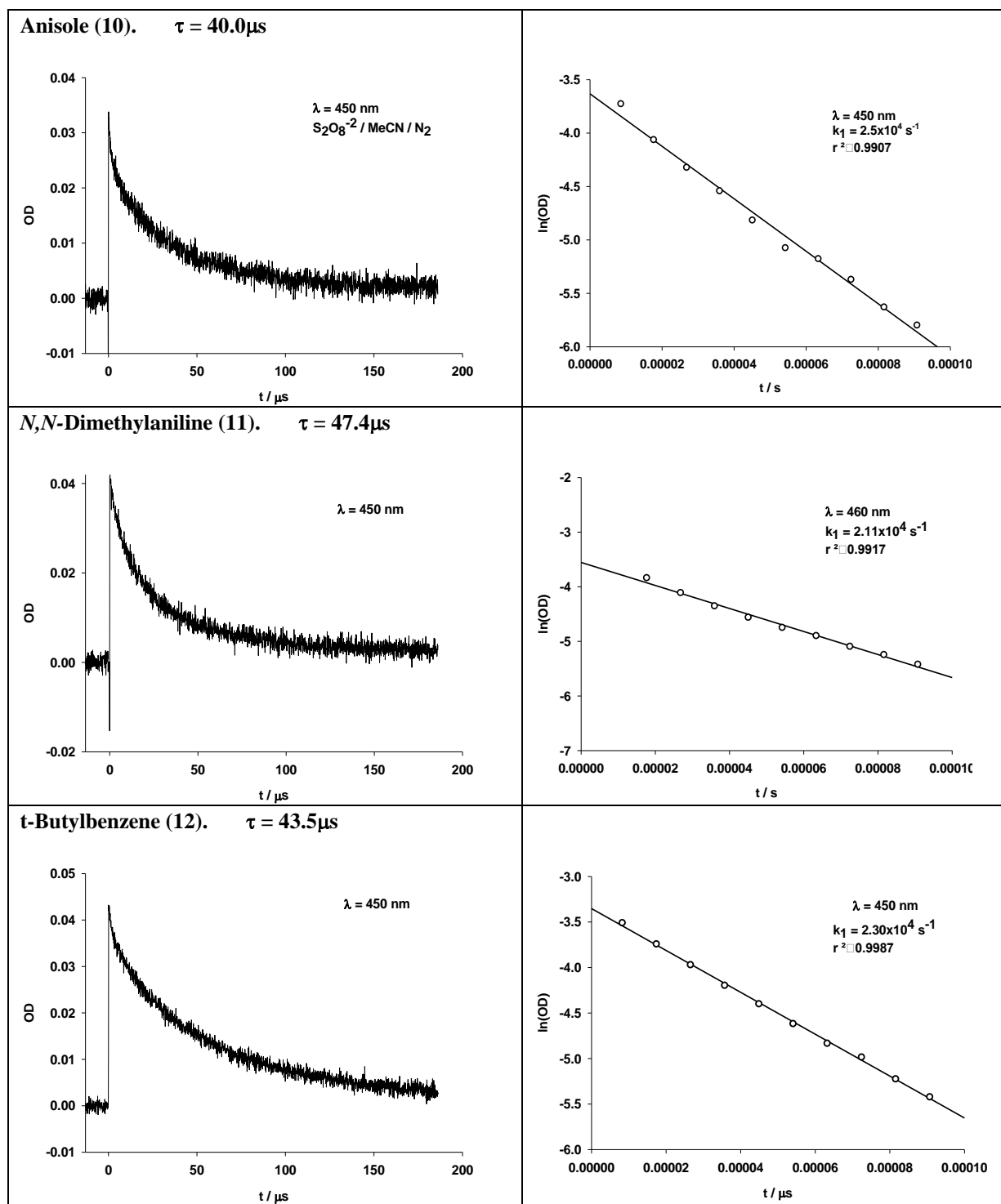


**Figure S2.** Transient decay traces and linear correlation plots for the determination of unimolecular rate constants ( $k_R$ ) of radical-cations of arylmesylate 1–4, aryl diethylphosphates 5–8, p-chloroanisole (9), anisole (10), N,N-dimethylaniline (11) and t-butylbenzene (12) in the presence of ammonium persulfate in MeCN/H<sub>2</sub>O (9:1) under N<sub>2</sub> atmosphere.

### 3. Solvent effect on the reaction rate constants of radical cations.

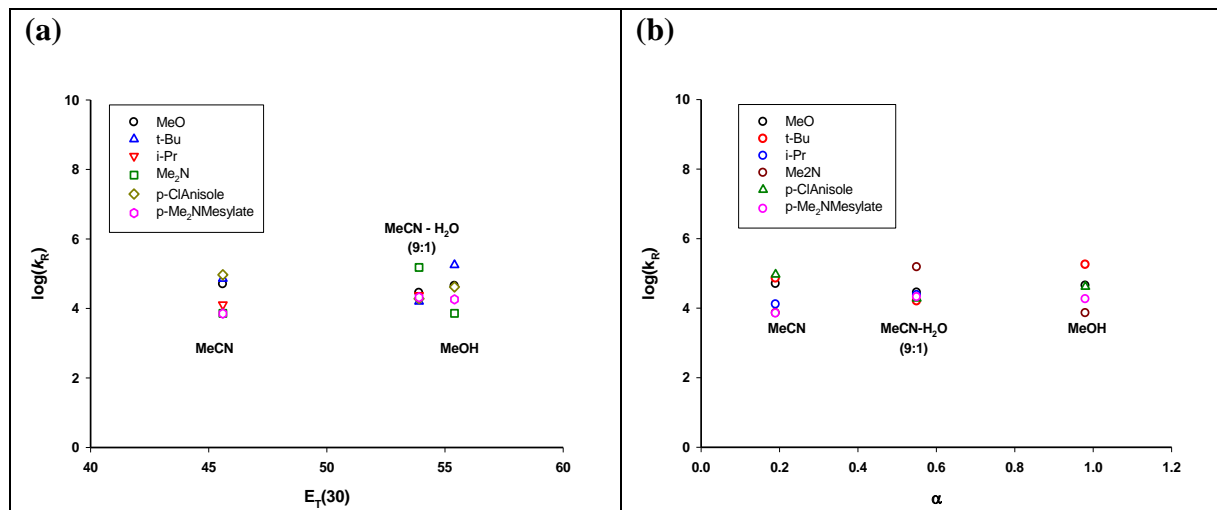


**Figure S3.** Correlation plots of  $\log(k_R)$  versus: (a) solvent polarity ( $E_T(30)$ ) parameter and (b) hydrogen bond donor ( $\alpha$ ) of radical cations  $4^{*+}$  -  $9^{*+}$ .

### 4. Hammett linear correlations of the reaction rate constants ( $k_R$ ) of radical cations and electron-transfer rate constants ( $k_{ET}$ ) of esters 1-8.

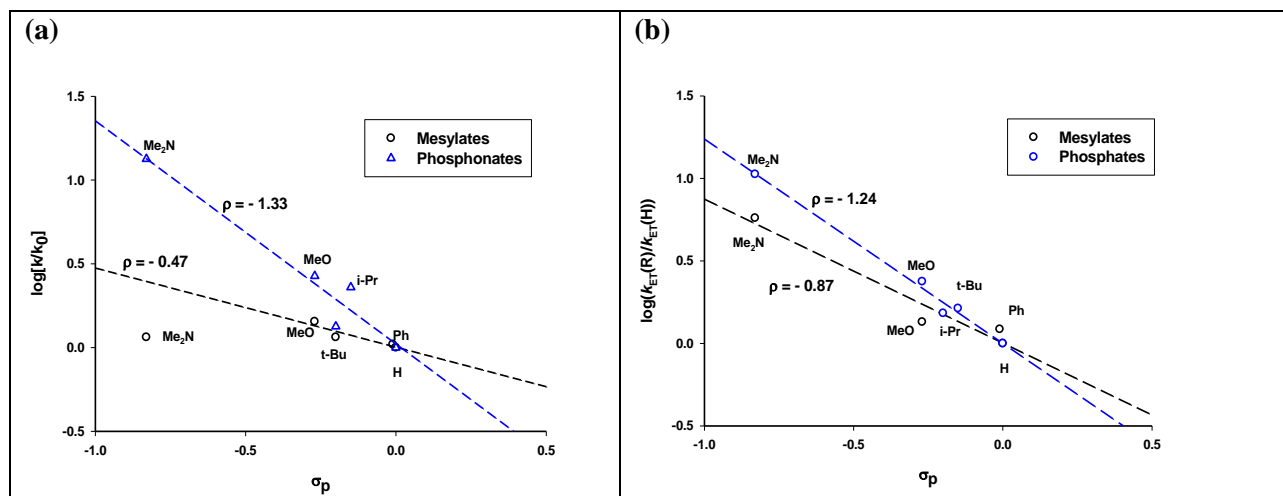


**Figure S4.** Hammett linear correlation of: (a) reaction rate constants of radical cations ( $k_R$ ) as  $\log(k/k_0)$  versus  $\sigma_p$ , and (b) electron-transfer rate constants of esters ( $k_{ET}$ ) as  $\log(k_{ET}(R)/k_{ET}(H))$  versus  $\sigma^+$ .



### 5. Quenching of radical cation decay traces by addition of increasing concentration of $\text{NaN}_3$ .

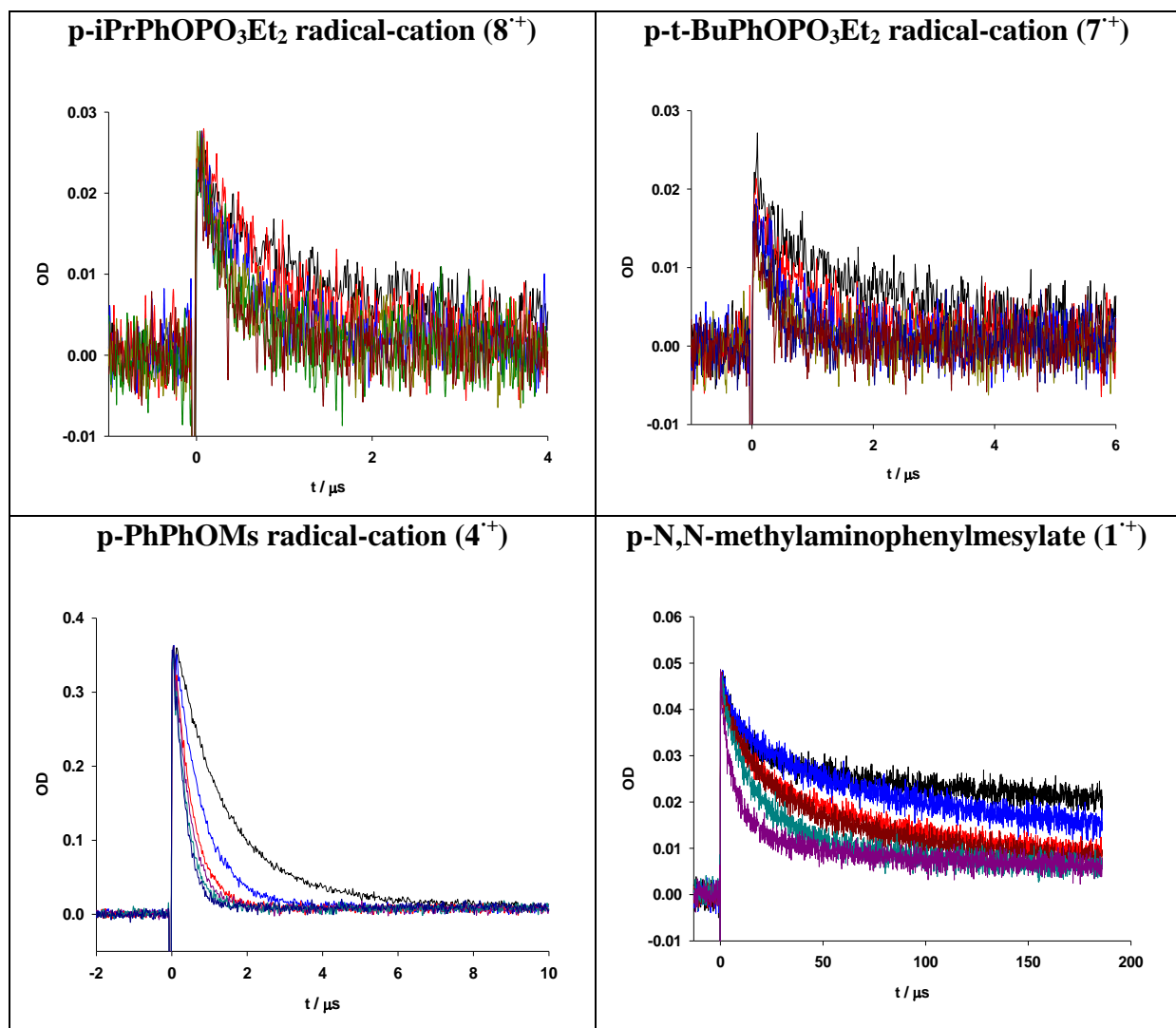


**Figure S5.** Quenching of radical cation decay traces recorded at the maximum absorption wavelength after a laser pulse (266 nm) in the presence of ammonium persulfate by addition of increasing concentration of  $\text{NaN}_3$  in acetonitrile water (9:1) mixture under  $\text{N}_2$  atmosphere.

## 6. Measurement of extinction coefficients ( $\epsilon$ ) and quantum yield of formation ( $\phi$ ) of radical cations and calculation of the electron-transfer rate constants ( $k_{ET}$ ).

*Measurement of extinction coefficients ( $\epsilon$ ) of radical cations  $\mathbf{1}^+$  -  $\mathbf{8}^+$ .* The extinction coefficients ( $\epsilon$ ) of radical cations  $\mathbf{1}^+$  -  $\mathbf{8}^+$  were measured by comparison with an internal standard with known extinction properties according to the methodology described in the literature.<sup>[S1]</sup> Thus, anisole (**10**) was selected as the adequate actinometer for measuring the  $\epsilon$  of the radical cations because possess well-known radical cation properties such as  $\epsilon(\mathbf{10}^+) = 3800 \text{ M}^{-1}\text{cm}^{-1}$  and  $\phi_{\text{ion}} = 0.60$ .<sup>[S2],[S3]</sup> Irradiation of ammonium persulfate solution in the presence of anisole with a laser pulse of 266 nm led to determine the concentration of anisole radical cation ( $\mathbf{10}^+$ ) because the extinction coefficient of  $\mathbf{10}^+$  is known. Thus, the concentration of sulfate radical anion ( $\text{SO}_4^{\cdot-}$ ) was estimated to be  $6.32 \times 10^{-6} \text{ M}$  assuming  $[\mathbf{10}^+] = [\text{SO}_4^{\cdot-}]$ . Then, the concentration of sulfate radical anion produced upon irradiation of ammonium persulfate in the presence of each selected ester (**1** – **8**) with a laser pulse (266 nm) was also estimated to be  $6.32 \times 10^{-6} \text{ M}$  because the experimental condition is the same that was employed with the actinometer anisole. Finally, the extinction coefficients  $\epsilon(\text{ester}^+)$  of each ester radical cation ( $\mathbf{1}^+$  -  $\mathbf{8}^+$ ) were easily calculated applying systematically the Lambert-Beer relationship according to equation 1,

$$\epsilon(\text{ester}^+) = \frac{\Delta(\text{OD})}{[\text{ester}^+]} = \frac{\Delta(\text{OD})}{(6.23 \times 10^{-6} \text{ M})} \quad (1)$$

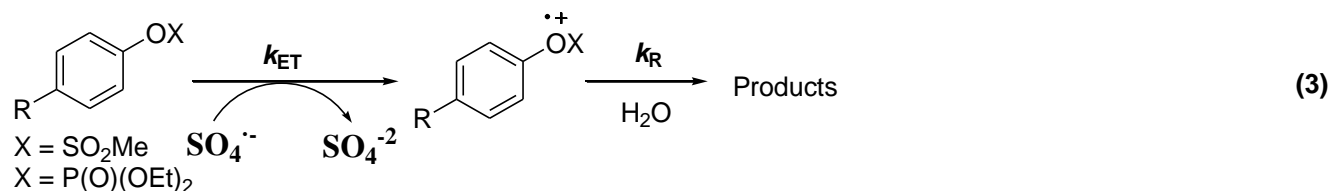
where  $\Delta(\text{OD})$  is the optical density of the ester radical cation ( $\text{ester}^+$ ) at zero time after the laser pulse and  $[\text{ester}^+]$  is the concentration of the ester radical cation. The applied methodology for the calculation of the extinction coefficients involved an electron transfer process between sulfate radical anion ( $\text{SO}_4^{\cdot-}$ ) and the ester (**1** – **8**) as well as with the actinometer anisole (**10**). The extinction

coefficients calculated for the first time according to equation (1) for radical cations  $\mathbf{1}^{\cdot+}$  -  $\mathbf{8}^{\cdot+}$  are collected in Table 1 (see main text). Noteworthy, *N,N*-dimethylaniline (**11**) was selected as a second actinometer in order to corroborate and to confirm that the concentration of sulfate radical cation ( $\text{SO}_4^{\cdot+}$ ) after a laser pulse of 266 nm was *ca.*  $10^{-6}$  M. Thus, irradiation of a solution of ammonium persulfate in the presence of *N,N*-dimethylaniline applying the same methodology as for anisole provided a  $\Delta(\text{OD})$  value of 0.029 at zero time after the laser pulse and knowing the extinction coefficient of  $\mathbf{11}^{\cdot+}$  of  $4500 \text{ M}^{-1}\text{cm}^{-1}$ <sup>[S4]</sup> the concentration of  $\text{SO}_4^{\cdot+}$  was calculated to be  $6.44 \times 10^{-6}$  M assuming again that  $[\text{SO}_4^{\cdot+}] = [\mathbf{11}^{\cdot+}]$ . Therefore, the consistency of the method was clearly verified using two distinct actinometers whose extinction coefficients were measured independently.

*Quantum yield of formation ( $\phi$ ) of radical cations  $\mathbf{1}^{\cdot+}$  -  $\mathbf{8}^{\cdot+}$ .* The quantum yields of ester free radical cation production ( $\phi$ ) were also measured for the first time and anisole (**10**) was again employed as the actinometer because the  $\phi$  value of anisole radical cation ( $\mathbf{10}^{\cdot+}$ ) has been previously measured and was found to be 0.60.<sup>[S3]</sup> The quantum yields were derived by relative actinometry. The acetonitrile water (9:1) mixture solutions of ammonium persulfate in the presence of the actinometer and in the presence of each ester (**1** – **8**) were optically matched solutions at 266 nm. Then, the UV-visible absorption spectra of the primary transient formed immediately after the laser pulse were recorded and the area of each absorption spectrum was calculated. Finally, the quantum yields of ester free radical cation production ( $\phi$ ) were easily calculated applying equation (2).

$$\phi(\text{ester}^{\cdot+}) = \phi(\mathbf{10}^{\cdot+}) \frac{\text{Area}(\text{ester}^{\cdot+})}{\text{Area}(\mathbf{10}^{\cdot+})} \frac{\epsilon(\mathbf{10}^{\cdot+})}{\epsilon(\text{ester}^{\cdot+})} = 0.60 \frac{\text{Area}(\text{ester}^{\cdot+})}{\text{Area}(\mathbf{10}^{\cdot+})} \frac{\epsilon(\mathbf{10}^{\cdot+})}{\epsilon(\text{ester}^{\cdot+})} \quad (2)$$

The  $\phi$  values thus obtained for each ester radical cation are also shown in Table 1 (see main text).  
*Calculation of the electron-transfer rate constants ( $k_{ET}$ ).* The electron-transfer rate constants  $k_{ET}$  were calculated from the quantum yields of free radical cation production ( $\phi$ ) considering the formation and reaction pathways of the ester radical cations according to equation (3).



Application of steady-state conditions to equation (3) the quantum yields of free radical cation production ( $\phi$ ) can be written in terms of  $k_R$  and  $k_{ET}$  that, after mathematical rearrangement, the final relationship between  $k_{ET}$  and  $\phi$  was obtained as can be seen in equation (4).

$$\phi = \frac{2 k_{ET} [\text{SO}_4^{\cdot-}]}{(k_R + 2 k_{ET} [\text{SO}_4^{\cdot-}])} \quad \Longrightarrow \quad k_{ET} = \frac{k_R \phi}{2 [\text{SO}_4^{\cdot-}] (1 - \phi)} \quad (4)$$

The last mathematical relationship certainly provides the  $k_{ET}$  rate constant values of the electron-transfer pathway between sulfate radical anion and the aryl mesylates and aryl phosphates, respectively, taking into account that the kinetic parameters ( $k_R$  and  $\phi$ ) and the concentration of  $\text{SO}_4^{\cdot-}$  are known. The  $k_{ET}$  values thus calculated are collected in Table 1 (see main text). Noteworthy, the electron-transfer rate constants  $k_{ET}$  of compounds **9** – **12** were also calculated applying the above described procedure and the  $k_{ET}$  values are also shown in Table 1 (see main text).

## 7. References.

- [S1] a) R. Lomoth, S. Naumov, O. Brede, *J. Phys. Chem. A* **1999**, *103*, 2641-2648; b) R. Lomoth, O. Brede, *Chem. Phys. Lett.* **1998**, *288*, 47–51; c) M. Hara, S. Tojo, T. Majima, *J. Photochem. Photobiol. A: Chem.* **2004**, *162*, 121–128.
- [S2] P. O'Neill, S. Steenken, D. Schulte-Frohlinde, *J. Phys. Chem.*, **1975**, *79*, 2773 – 2779.
- [S3] A. Lewandowska, G. L. Hug, G. Hoener, T. Pedzinski, P. Filipiak, B. Marciniak. *Chem. Phys. Lett.*, **2010**, *11*, 2108.
- [S4] a) H. C. Christensen, *Int. J. Radiat. Phys. Chem.*, **1972**, *4*, 511; b) H. C. Christensen, K. Schessted, E. J. Hart, *J. Phys. Chem.*, **1973**, *77*, 983.